Biochimica et Biophysica Acta 1817 (2012) 1576–1587

Contents lists available at SciVerse ScienceDirect

Biochimica et Biophysica Acta

journal homepage: www.elsevier.com/locate/bbabio

Spectroscopic studies of two spectral variants of light-harvesting complex 2 (LH2) from the photosynthetic purple sulfur bacterium *Allochromatium vinosum*

Dariusz M. Niedzwiedzki [a,d,*], David Bina [c,d], Nichola Picken [b], Suvi Honkanen [b], Robert E. Blankenship [a,c,d], Dewey Holten [a,d], Richard J. Cogdell [b]

[a] Photosynthetic Antenna Research Center, Washington University in St Louis, MO 63130, USA
[b] Biomedical Research Building, Institute of Biomedical and Life Sciences, University of Glasgow, Glasgow, UK
[c] Department of Biology, Washington University in St Louis, MO 63130, USA
[d] Department of Chemistry, Washington University in St Louis, MO 63130, USA

ARTICLE INFO

Article history:
Received 27 February 2012
Received in revised form 8 May 2012
Accepted 22 May 2012
Available online 31 May 2012

Keywords:
Time-resolved spectroscopy
Photochemistry of carotenoids
Light harvesting complex 2
Bacteriochlorophyll *a*
Energy transfer

ABSTRACT

Two spectral forms of the peripheral light-harvesting complex (LH2) from the purple sulfur photosynthetic bacterium *Allochromatium vinosum* were purified and their photophysical properties characterized. The complexes contain bacteriochlorophyll *a* (BChl *a*) and multiple species of carotenoids. The composition of carotenoids depends on the light conditions applied during growth of the cultures. In addition, LH2 grown under high light has a noticeable split of the B800 absorption band. The influence of the change of carotenoid distribution as well as the spectral change of the excitonic absorption of the bacteriochlorophylls on the light-harvesting ability was studied using steady-state absorption, fluorescence and femtosecond time-resolved absorption at 77 K. The results demonstrate that the change of the distribution of the carotenoids when cells were grown at low light adapts the absorptive properties of the complex to the light conditions and maintains maximum photon-capture performance. In addition, an explanation for the origin of the enigmatic split of the B800 absorption band is provided. This spectral splitting is also observed in LH2 complexes from other photosynthetic sulfur purple bacterial species. According to results obtained from transient absorption spectroscopy, the B800 band split originates from two spectral forms of the associated BChl *a* monomeric molecules bound within the same complex.

1. Introduction

Light harvesting complex 2 (LH2) is one of the two types of transmembrane photosynthetic antenna complexes present in the photosynthetic apparatus in purple bacteria. To date, only two high-resolution structures of the LH2 antenna complex have been determined using X-ray crystallography. These were isolated from two non-sulfur purple bacterial species: *Rhodopseudomonas (Rps.) acidophila* strain 10050 and *Phaeospirillum (Phs.) molischianum*. The complexes were determined to ~2.5 Å resolution, though the LH2 from *Rps. acidophila* was later improved to 2.0 Å [1–4]. These structures show that the complexes form circular aggregates consisting of eight (*Phs. molischianum*) or nine (*Rps. acidophila*) identical protein subunits formed by heterodimers of polypeptide chains, denoted α and β with transmembrane orientation. The α/β subunits form a double ring with inner and outer diameters of 36 Å and 68 Å for *Rps. acidophila,* respectively, and 31 Å and 62 Å for *Phs. molischianum*. Each protein subunit binds three bacteriochlorophylls *a* (BChl *a*). The strongly coupled BChl *a* molecules have their bacteriochlorin rings oriented perpendicular to the membrane plane and interact excitonically producing a combined Q_y transition in the vicinity of 850 nm. They form a ring with closest distances between molecules of 3.66 Å for *Rps. acidophila* and 3.54 Å for *Phs. molischianum* in the dimers (a pair of B850 bacteriochlorophylls from α and β subunits) and 3.74 Å and 3.63 Å, respectively, between molecules from neighboring dimers. The monomeric BChl *a* molecules (B800) are oriented so that their tetrapyrole rings lie parallel with the membrane plane and are positioned between β–polypeptides [1–3]. In complexes from both species, each α/β subunit contains also one carotenoid. This is rhodopin glucoside in *Rps. acidophila* and lycopene in *Phs. molischianum*. Due to the same number of conjugated carbon-carbon double bonds in the backbone these carotenoids possess similar spectroscopic properties regardless of the differences in the terminal substituents [5].

In contrast, very little structural information is available for LH2 complexes from purple sulfur bacteria due to partial or incomplete information about primary sequences of their LH2 peptides, as well as difficulties in growing many types of these bacterial cultures. Recently, some progress with structural studies on these complexes was achieved using electron microscopy (EM) [6]. The EM of single LH2 complexes from

* Corresponding author at: Photosynthetic Antenna Research Center, Washington University in St. Louis, St. Louis, MO 63130, Campus Box 1138, USA. Tel.: +1 314 935 8483; fax: +1 314 935 4925.
E-mail address: niedzwiedzki@wustl.edu (D.M. Niedzwiedzki).

0005-2728/$ – see front matter © 2012 Elsevier B.V. All rights reserved.
doi:10.1016/j.bbabio.2012.05.009

Allochromatium (Alc.) vinosum (formerly *Chromatium vinosum*) revealed that the complex adopts two circular forms, the dominant form built from 13 α/β subunits and a minor form that was shown to consist between 10 and 12 α/β subunits. Based on these statistical projections the outer ring size of the LH2 may vary from 68 to 115 Å [6]. Despite the fact that EM revealed at least two structural forms of the LH2 it was not clear from preparative point of view whether that sample contained more than one type of LH2 complex or not. Nevertheless it is clear that LH2 complexes from sulfur purple bacteria may have different ring sizes compared to their "non-sulfur" counterparts. These structural differences are also reflected in spectroscopic properties. The steady-state electronic absorption spectrum of LH2 complexes from some purple sulfur bacteria grown under normal light conditions show an abnormally broad B800 band, not observed in LH2 complexes from non-sulfur species. Moreover, upon lowering the temperature the B800 band splits into two distinct peaks separated by ~15 nm with almost equal amplitudes [7,8].

Different explanations have been offered for the B800 band splitting. One assumes that the sample is actually a mixture of two spectrally slightly different LH2 complexes that are impossible to separate by the normal biochemical purification procedures [7]. The second hypothesis supported by polarized time-resolved absorption spectroscopy presumes that this LH2 contains two sets of B800 molecules, equivalently distributed within the individual LH2 complex [9]. A possible third hypothesis is that the B800-type BChl *a* molecules are organized as excitonically coupled molecules that give rise to a splitting of the absorption band. The equal intensities of the two absorption bands around 800 nm would indicate, in this model, that the oscillator strength is evenly distributed between two exciton components of the coupled monomers [10].

Bacteria that produce LH2 with a split B800 band like *Alc. vinosum* or *Thermochromatium (Tch.) tepidum* express multiple types of α-and β-apoproteins [11]. Under such circumstances, it is easy to imagine that individual LH2 rings with an inhomogeneous polypeptide composition could result in the second scenario mentioned above. Moreover, if the LH2 could be composed from randomly assembled multiple types of α/β subunits, the spectral properties of the B800-type BChls may differ even within the same LH2 complex.

In order to obtain a definitive answer to this issue we applied femtosecond time-resolved transient absorption spectroscopy at 77 K on these two spectral forms of the LH2 complex from *Alc. vinosum*. One of the forms denoted as Thio-HL (high light) contains the characteristic split B800 band at 77 K, the second form denoted as Sulph-LL (low light) has typical "non-sulfur" character with one sharp B800 peak. In addition, both complexes have different absorption spectra in the region where the carotenoids absorb. We also evaluated how changes in the carotenoid composition affect the path of energy flow in these antenna complexes.

2. Materials and methods

2.1. Bacteria growth and LH2 complex preparation

The cells were grown anaerobically in the light in the presence of either sodium sulfide or sodium thiosulfate as the sources of reduced sulfur [12,13]. The cells grown at high light (220 lux, Osram incandescent 150 watt bulbs) with sodium thiosulphate at 30 °C produced the LH2 with the double B800 band while those grown with sodium sulphide at low light (10 lux, Osram incandescent 60 watt bulbs) and at 30 °C produced the LH2 complex with a single B800 peak. After growth, the cells were harvested by centrifugation, resuspended in 20 mM Tris HCl pH 8.0 and broken by passage through a French Press at 10 tons/sq. inch in the presence of a little DNAse. The chromatophore membranes were then pelleted by centrifugation and resuspended in 20 mM Tris HCl buffer pH 8.0 to an OD at 850 nm of 50. The membranes were then solubilized with the addition of 2% DDM (n-Dodecyl-beta-D-maltopyranoside) for 4 hours while stirring at room temperature. Any unsolubilized material was then removed by a brief centrifugation and the LH complexes fractioned by sucrose density centrifugation for 16 hours at 150,000*g* at 4 °C. The sucrose step gradient was made up of 0.6, 0.8, 1.0 and 1.2 M sucrose steps in 20 mM Tris HCl buffer with 0.02% DDM. The LH2 complexes where removed from the gradients and further purified by a combination of ion exchange and molecular sieve chromatography.

2.2. Carotenoid separation and purification

Carotenoids were extracted by applying a mixture of 1:1 (v/v) acetone:methanol to concentrated LH2 complexes. Carotenoids were separated from the extract by adding small volume of *n*-hexane and partitioning with water. The *n*-hexane layer containing carotenoids was then injected to an Agilent 1100 HPLC system employing a LiChrosorb Silica normal phase column (ES Industries) (250 mm × 4.6 mm) with isocratic flow rate of 1.5 mL/min and *n*-hexane:tetrahydrofuran (90:10, v/v) as a mobile phase. The chromatograms were monitored at wavelengths corresponding to the (0-0) vibronic band of the carotenoids steady-state absorption observed in the applied solvent mixture.

2.3. Steady-state absorption and fluorescence spectroscopy

The samples of the LH2 were diluted in 20 mM Tris-HCl buffer, pH 8 with 0.02% DDM in order to perform room temperature (RT) measurements. For 77 K measurements buffer containing 57% glycerol (v/v) in 20 mM Tris–HCl (pH 8) with 0.02% DDM was used. Low temperature experiments were performed using OptistatDN cryostat (Oxford Instruments, UK). Steady-state absorption and fluorescence spectra were recorded in 1 cm path length cuvettes using a Perkin-Elmer Lambda 950 spectrometer and a Photon Technology International fluorimeter, respectively. Fluorescence was detected at a right angle with respect to the excitation beam and corrected for the instrument response. The sample OD was adjusted to 0.1 at the maximum of the B850 absorption band. Fluorescence excitation spectra were corrected for instrument excitation characteristics using a calibrated reference photodiode. The bandpass for the fluorescence measurements was set to 4 nm.

2.4. Femtosecond time-resolved absorption spectroscopy

Time-resolved pump-probe absorption experiments were carried out using Helios, a femtosecond transient absorption spectrometer from Ultrafast Systems, LCC coupled to a femtosecond laser system. It consists of Solstice, a one box ultrafast amplifier (Spectra-Physics) built of Spitfire Pro XP, a Ti:sapphire regenerative amplifier with a pulse stretcher and compressor, Mai-Tai, a femtosecond oscillator as seeding source and Empower, a diode-pumped solid state pulsed green laser as the pump source. The system produces pulses centered at 800 nm with energy of ~3.5 mJ, ~90 fs duration and 1 kHz repetition rate. Ninety percent of the output beam was used to generate a pump beam in Topas-C, an optical parametric amplifier equipped with Berek extension (Light Conversion Ltd, Lithuania). The remaining 10% was used to produce probe pulses in the Helios spectrometer. A white light continuum probe in the visible (VIS) region was generated by a 3 mm thickness Sapphire plate. A near infra-red (NIR) probe was generated using 10 mm thickness proprietary crystalloid rod. A complementary metal–oxide–semiconductor (CMOS) linear sensor with 1024 pixels was used as a detector in the VIS range and a 256 pixel InGaAs linear diode array in the NIR. To provide an isotropic excitation of the sample and avoid pump-probe polarization effects the pump beam was depolarized. For carotenoids in 2-MTHF the energy of the pump beam was set to 1 μJ with a spot size of 1 mm diameter, corresponding to intensity between 3.4 and 3.5×10^{14} photons/cm^2 depending on the exact excitation wavelength. In order to minimize excited state annihilation processes in the LH2, the energy of the pump was kept between 0.06

and 0.25 μJ, corresponding to intensity between 2 and 3.4×10^{13} photons/cm^2, depending on the excitation wavelength used. To assure that LH2s will not spontaneously aggregate in the glycerol/buffer mixture, the DDM concentration was raised to 0.04%, well above the critical micelle concentration of that detergent in water (0.009%). The optical densities (OD) of the samples (in the region of the carotenoid band) were adjusted to 0.5 in 4 mm path length cuvettes. In order to achieve selective excitation of 790 nm and 810 nm sub-peaks of the B800 band in the HL form, the excitation beam was filtered with 780 nm and 810 nm interference filters with 10 nm bandwidth.

2.5. Transient absorption data analysis and fitting

Group velocity dispersion of the transient absorption (TA) datasets was corrected using Surface Explorer (v. 2.0) from Ultrafast Systems LCC by building a dispersion correction curve based on the set of initial times of transient signals obtained from fits of representative kinetics. Global fitting analysis of the datasets was performed using ASUfit 3.0, software provided by Dr. Evaldas Katilius at Arizona State University (http://www.public.asu.edu/~laserweb/asufit/asufit.html), with some modifications. The full width at half maximum of a temporal response function was calculated as one of the parameters of the fitting procedure. Fitting was done using an unbranched, unidirectional decay path model (A→B→C→D→…) that assumes that back-reactions can be ignored on the assumption that the energy losses are large enough such that the reverse reaction rates are negligible [14]. Because the excited states decay path of carotenoids can be very adequately characterized by sequence, the applied model gives not only rate constants (these are independent of the fitting model) but also spectral characteristics of species (excited states) involved in the decay and not just amplitudes of the pre-exponential factors.

3. Results

3.1. Steady-state spectroscopy

Fig. 1 presents the steady-state absorption (converted to $1-T$, where T is the transmittance), fluorescence emission (Em) and fluorescence excitation (Ex) spectra of the Thio-HL and Sulph-LL forms of the LH2 complex from *Alc. vinosum*. Both forms of the LH2 complex exhibit the common features typical of the peripheral antenna from purple bacteria. These features include BChl *a* bands associated with different absorptive transitions: Soret (380 nm), Q_x (590 nm), Q_y monomeric at 800 nm and Q_y excitonic at 850 nm (commonly referred to as B800 and B850) as well as carotenoid absorption bands in the region of 420–550 nm. However, several differences are readily noticeable. At room temperature, the Q_y BChl *a* bands peak at 796 nm and 847 nm in the Thio-HL form (Fig. 1a), while in the Sulph-LL form they are shifted to longer wavelengths, and have maxima at 803 nm and 856 nm (Fig. 1c). Moreover, both B800 and B850 bands appear broadened in the Thio-HL form compared to the Sulph-LL form.

Lowering the temperature to 77 K results in splitting of the B800 band in the Thio-HL form with two peaks appearing at 792 and 806 nm (Fig. 1b). This phenomenon was observed previously for an LH2 preparation from the purple sulfur bacterium *Thermochromatium (Tch.) tepidum* [7,15] as well as for an LH2 sample from the species of bacterium studied here [6,8]. The B850 band shifts to longer wavelengths by about 20 nm. In the Sulph-LL complex (Fig. 1d), a substantial increase of intensity of the B800 band occurs relative to the B850 band, also a small feature at 767 nm is clearly visible. In the Sulph-LL form low temperature induces a spectral shift of the B850 band by ~10 nm to longer wavelengths.

At room temperature, the maximum of the carotenoid absorption band appears at about 488 nm in the Thio-HL LH2 and at 500 nm in the Sulph-LL form (Fig. 1a, c). At 77 K (Fig. 1b, d), resolution of the vibronic peaks in the carotenoid absorption band is enhanced and the spectra clearly indicate the presence of several different types of carotenoids in each of these complexes as well a noticeable difference of carotenoid composition between them.

Comparison of the $1-T$ (black lines) and the fluorescence excitation (blue lines) profiles allows calculation of the efficiency of energy transfer (EET) from carotenoids to BChl *a* in both complexes. The profiles were normalized in the B850 band, assuming a 100% EET for direct excitation of the B850 BChl *a* molecules at this wavelength. The Car-to-BChl *a* EETs were calculated at carotenoid second vibronic band (see Fig. 1), which is least affected by the tails of BChl *a* transitions (Soret and Q_x). The Car-to-BChl *a* EET is very similar for both complexes (36–40%) and very weakly depends on temperature (Fig. 1). The efficiency of the energy transfer from the sub-bands of the B800 band in the Thio-HL complex to B850 was approximately the same ~95% for both components.

3.2. Carotenoid composition

Both antenna complexes show a mixed carotenoid composition; however, there are significantly different proportions of individual carotenoids in the two cases. Both LH2s contain five types of open chain carotenoids with carbon-carbon double bond conjugation length (N) of 11 (lycopene, rhodopin), 12 (anhydrorhodovibrin, rhodovibrin) and 13 (spirilloxanthin). In the Thio-HL form, rhodopin is the dominant component and accounts for 75% of all carotenoids present. In the Sulph-LL form the distribution of various carotenoids is more balanced and a significant reduction in the quantity of the short conjugation-length carotenoids ($N=11$) is observed. The most dominant (30%) is anhydrorhodovibrin ($N=12$), which together with the spectrally almost identical rhodovibrin ($N=12$) account for almost half of the carotenoid pool (Table 1). The absorption spectra of three representative carotenoids taken in *n*-hexane are shown in Fig. 2 along with their molecular structures. The fact that the spectra show a pronounced cis peak in the ~350 nm region does not mean that the studied LH2 complexes contain *cis* isomers. This is unlikely true and presence of *cis* isomers is simply the result of a spontaneous isomerization from the all-*trans* form during extraction of the molecules from the LH2 complexes and processing them for HPLC. The

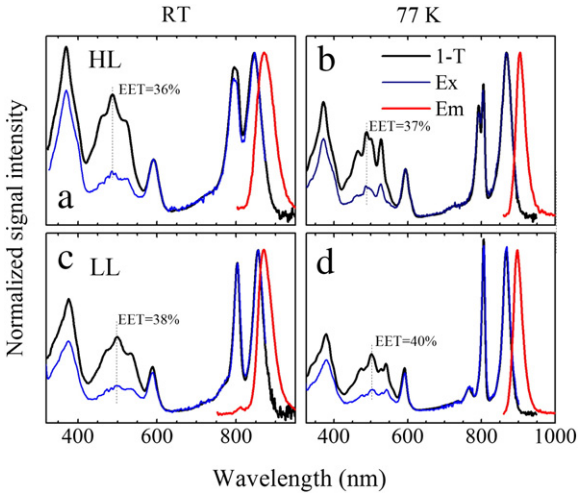

Fig. 1. (a, c) Room temperature and (b, d) 77 K steady-state absorption (expressed as $1-T$, where T is transmittance), fluorescence (Em) and fluorescence excitation (Ex) spectra of the LH2 complex from the purple sulfur bacterium *Alc. vinosum*. The spectra were normalized at Q_y band of B850 BChl *a*. The efficiency of energy transfer (EET) obtained by direct division of Exc over $1-T$ at the points having the least spectral contribution from BChl *a* gives the Car→BChl *a* EET of 36 and 37% (RT, 77 K) for the HL LH2 and 38, 40% (RT, 77 K) for the LL LH2.

Table 1
Partial content of the carotenoids present in the HL and LL forms of the LH2 complex from *Alc. vinosum*.

Carotenoid	HL LH2	LL LH2
Lycopene ($N=11$)	6	13
Anhydrorhodovibrin ($N=12$)	6	30
Spirilloxanthin ($N=13$)	4	19
Rhodopin ($N=11$)	75	22
Rhodovibrin ($N=12$)	9	15
Total	**100**	**100**

spectra of rhodovibrin and lycopene are very similar to their counterparts with the same *N* and were omitted for the sake of clarity. It is clear that the shift of carotenoid distribution from carotenoids with $N=11$ to those with longer conjugation ($N=12$ and 13) is a source of the observed differences in carotenoid's absorption spectra band in the two types of the LH2.

3.3. Transient absorption studies of isolated carotenoids

In order to fully understand the role of individual carotenoids in the complexes comparative ultrafast 77 K transient absorption (TA) studies of the carotenoids in 2-MTHF glasses and bound to the LH2 complexes in glycerol/buffer (1:1 v/v) were performed. As representative compounds, rhodopin and anhydrorhodovibrin were chosen since these two pigments are the major components in the carotenoid distributions of the LH2 complexes. Lycopene is almost spectrally indistinguishable from rhodopin and conclusions drawn from the results obtained for rhodopin can be applied also to this carotenoid. Similar argumentation can be applied for rhodovibrin and anhydrorhodovibrin. Finally, spirilloxanthin was omitted from the analysis because this carotenoid was previously studied in detail in LH1 from *R. rubrum*, LH2 from *Alc. vinosum* at RT as well in 2-MTHF at 77 K [16–18]. The prior results demonstrated that for spirilloxanthin only the $S_2(1^1B_u^+)$ state participates significantly in energy transfer to BChl *a*.

Fig. 3 shows results of TA of rhodopin frozen to 77 K in 2-MTHF. The TA spectra taken at different delay times are given in Fig. 3a. The carotenoid was excited in its (0-0) vibronic band at 528 nm (18,940 cm^{-1}). This excitation causes an instantaneous ground state bleaching visible as a negative spectral feature. Accompanying the ground state bleaching, a positive signal appears in the NIR

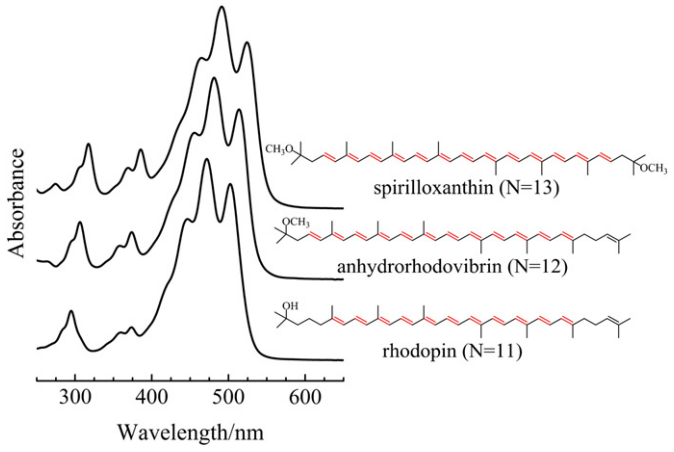

Fig. 2. Steady-state absorption and molecular structures of three representative open chain carotenoids present in the LH2 from *Alc. vinosum*: rhodopin, anhydrorhodovibrin and spirilloxanthin. The *N* numbers given in parenthesis indicate the number of conjugated carbon–carbon bonds and are marked on the structure in red. The spectra were taken in *n*-hexane at room temperature.

range with maximum at 1,160 nm (8,620 cm^{-1}) (Fig. 3b) and disappears within several hundreds of femtoseconds. This time evolution is associated with the appearance of a positive ΔA reflecting transient absorption from the $S_2(1^1B_u^+)$ state [19,20]. Subsequently (TA spectra after 1 and 5 ps), a sharp positive band appears in the VIS range at 585 nm (17,080 cm^{-1}). This band was observed for a number of carotenoids and is well-known to be associated with an absorption transition occurring from the first excited singlet state and is commonly assigned to $S_1(2^1A_g^-) \rightarrow S_n$, where S_n is a higher excited singlet electronic state with a B_u-like symmetry (Polivka has reviewed these carotenoid absorption characteristics [21].) Simultaneously to the $S_1(2^1A_g^-) \rightarrow S_n$ transition, another transient absorption band is also visible in the NIR range (Fig. 3b, TA spectra after 1 and 4 ps). This has a three-peak shape (two of the peaks are at 1,320 and 1,595 nm (7,560 and 6,275 cm^{-1})) somewhat similar to ground state steady-state absorption. This multi-feature spectral characteristic was previously recorded for a number of carotenoids and based on its temporal properties was assigned to the $S_1(2^1A_g^-) \rightarrow S_2(1^1B_u^+)$ absorption transition [16,22,23].

The results of global fitting of the TA datasets are presented in Fig. 3c (VIS) and d (NIR). The amplitude spectra were obtained from a sequential decay path model, commonly called EADS (Evolution Associated Difference Spectra) [14]. The time constants values obtained from the fitting (excited-state lifetimes) are independent of the applied model; however, if an adequate fitting model is chosen (that mimics a real decay path) the spectral profiles reflect spectral characteristics of the pure molecular species abbreviated commonly as SADS (Species Associated Difference Spectra) [14]. Previous studies have shown that in case of some carotenoids, the sequential decay of excitation is very realistic and EADSs may be assumed as SADSs but this is not a general rule and often more advanced target modeling must be applied [14,24–28].

In the VIS range three kinetic components were sufficient for a satisfactory fit of the time profile, while in the NIR only two were required. The 260 fs lifetime associated with the first EADS component in the NIR range represents the lifetime of the $S_2(1^1B_u^+)$ state. The counterpart EADS from the VIS range is obscured by solvent response and is not shown. The EADS with lifetime of 600 fs in the visible region has a shape that has been previously associated with thermal relaxation from a non-relaxed $S_1(2^1A_g^-)$ state [24,27,29–33]. This typically appears on the long wavelength side of the main transient peak. The decay time constant of 5.3 ps (VIS) (5.2 ps in the NIR) of the second EADS is the lifetime of the thermally relaxed $S_1(2^1A_g^-)$ excited singlet state. The origin of the last EADS with decay time constant of 12 ps is still under debate and has been previously attributed to either absorptive transition from unknown excited singlet state, so-called S* and lying in the vicinity of the $S_1(2^1A_g^-)$ [28,34], from the $S_1(2^1A_g^-)$ state of a molecule in twisted conformation, or from a non-equilibrated ground state $S_0(1^1A_g^-)$ [27]. However, recent transient absorption studies performed on β-carotene and rhodopin glucoside with narrowband excitation has shown convincingly that S* is associated with an excited state [34]. The representative kinetics with corresponding fits are given in Fig. 3e and f.

The fact that both the $S_0(1^1A_g^-) \rightarrow S_2(1^1B_u^+)$ ground state absorption and $S_1(2^1A_g^-) \rightarrow S_2(1^1B_u^+)$ excited state absorption are known allows determination of the energy of a "dark state", $S_1(2^1A_g^-)$, that is simply a value required to bring both spectra to the best peak-valley overlay [22]. For rhodopin at 77 K this is 12,650 ± 50 cm^{-1}, which is only slightly larger compared to 12,450 cm^{-1} previously obtained in *n*-hexane at room temperature [15]. However, the values of the $S_1(2^1A_g^-)$ lifetime at RT in *n*-hexane and at 77 K in 2-MTHF are significantly different (3.3 ps at RT and 5.3 ps at 77 K).

The TA spectra of anhydrorhodovibrin taken at 77 K at different delay times, upon excitation at 544 nm (18,380 cm^{-1}) (into the (0-0) vibronic band of steady-state absorption) are shown in Fig. 4a. These spectral profiles are very similar to those observed for rhodopin but

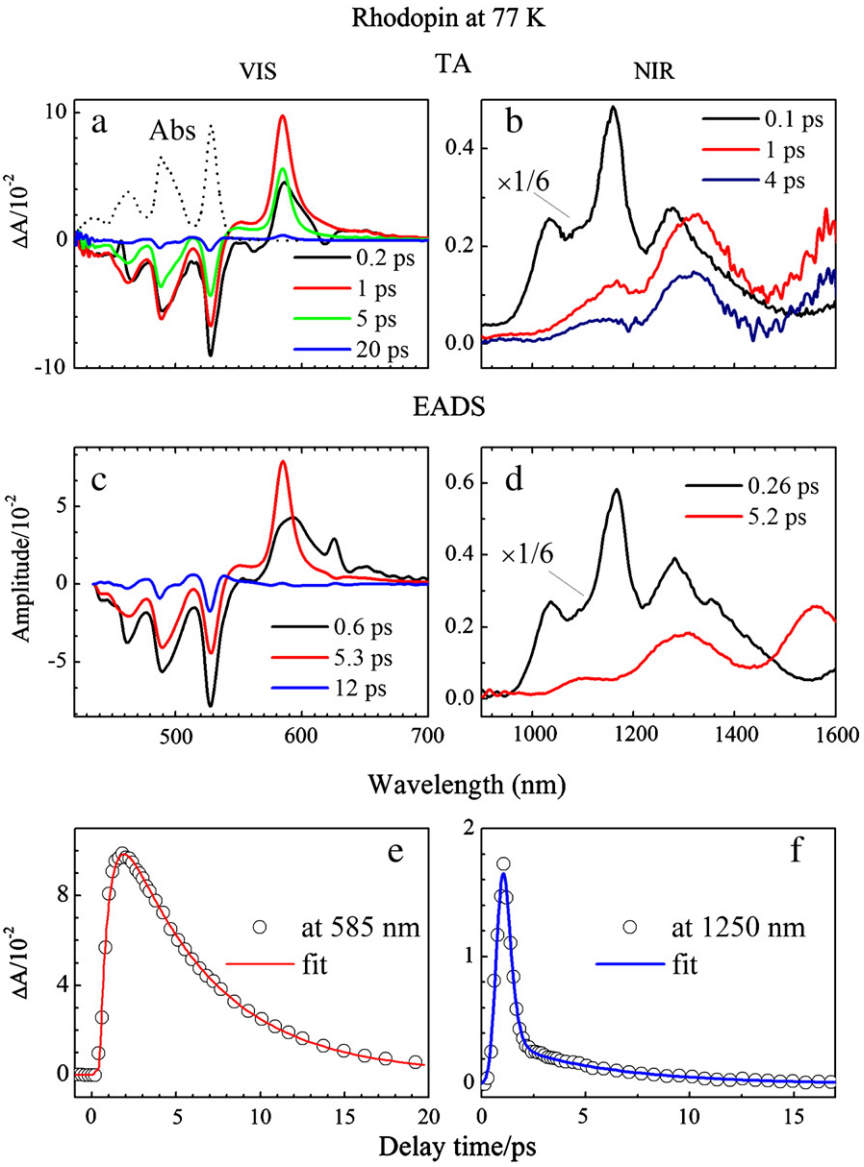

Fig. 3. (a) The steady-state (Abs) and transient absorption spectra (TA) of rhodopin ($N = 11$) taken at different delay times in the VIS and (b) NIR ranges at 77 K in 2-MTHF glass; (c) The results of global fitting obtained from sequential decay path model of TA spectra taken in VIS and in (d) NIR ranges; (e) The representative TA kinetics taken in the VIS and NIR ranges accompanied by fits obtained from global fitting.

with differences visible in positions of the transient bands. The subpicosecond TA band in the NIR range associated with absorptive transition from the $S_2(1^1B_u^+)$ state has maximum at around 1230 nm (8130 cm^{-1}) (Fig. 4b). The sharp $S_1(2^1A_g^-) \rightarrow S_n$ band appears at 602 nm (16,610 cm^{-1}) (Fig. 4a). The $S_1(2^1A_g^-) \rightarrow S_2(1^1B_u^+)$ transition shows two distinctive peaks at 1290 and 1,560 nm (7,750 and 6,410 cm^{-1}). The EADS profiles and lifetimes resulting from global fitting of the TA datasets are presented in Fig. 4c (VIS) and d (NIR). As with rhodopin, the VIS datasets required three kinetic fitting components while the NIR data only two. The 160–270 fs EADS observed in the VIS and NIR ranges is associated with the transition from the $S_2(1^1B_u^+)$ state. The variation in the $S_2(1^1B_u^+)$ lifetime value observed in both ranges is most probably associated with the difference in instrument response in the two spectral regions. Lifetimes of the kinetic component associated with the $S_1(2^1A_g^-) \rightarrow S_n$ and $S_1(2^1A_g^-) \rightarrow S_2(1^1B_u^+)$ transitions match very well and are 3.1 and 3.2 ps respectively. The last EADS visible in the VIS range with the decay time constant of 12 ps is associated with the same type of spectral feature as that observed for rhodopin (S*). The representative kinetics, with corresponding fits, are given in Fig. 3e and f. The $S_1(2^1A_g^-)$ state energy of rhodopin at 77 K, obtained by overlaying the $S_1(2^1A_g^-) \rightarrow S_2(1^1B_u^+)$ and $S_0(1^1A_g^-) \rightarrow S_2(1^1B_u^+)$ spectral profiles is 11,600 ± 100 cm^{-1}.

3.4. Transient absorption studies of LH2 complexes

Fig. 5a shows the TA spectra of the Thio-HL LH2 from *Alc. vinosum* taken at different delay times in the VIS and NIR ranges at 77 K. The sample was excited into the carotenoid band at 520 nm (that preferably excites rhodopin). In addition to the spectral features well known for this molecule from the TA spectra in 2-MTHF glass, such as the ground state bleaching and excited state absorption bands associated with the $S_1(2^1A_g^-)$ state, bleaching of the B800 and B850 bands is also observed. Since this excitation wavelength does not excite BChl *a* directly it is apparent that intermolecular Car-to-BChl *a* energy transfer must occur. An additional spectral feature that is not observed in 2-MTHF is a long lived carotenoid bleaching, accompanied with weak transient absorption band appearing at ~574 nm (18,270 cm^{-1}). This absorptive transition is associated with a carotenoid excited triplet

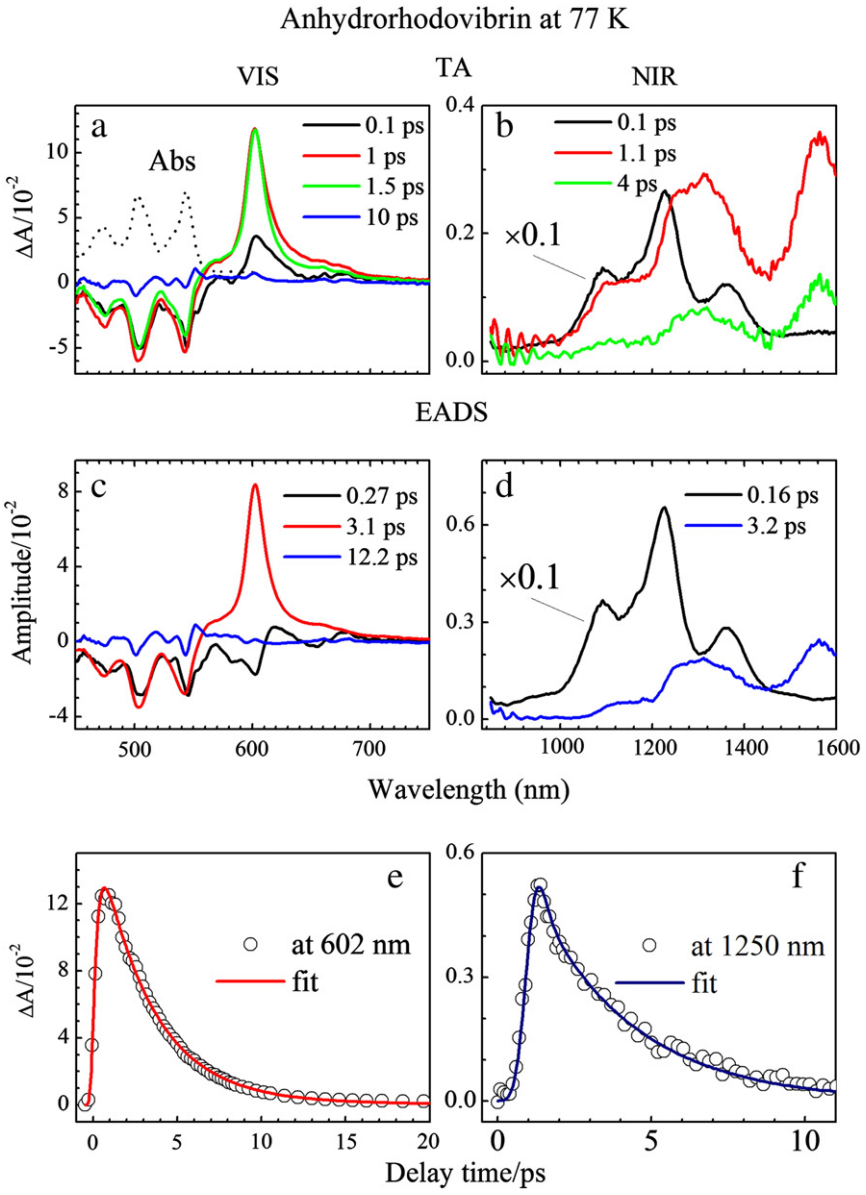

Fig. 4. (a) The steady-state (Abs) and transient absorption spectra (TA) of anhydrorhodovibrin ($N = 12$) taken at different delay times in the VIS and (b) NIR ranges at 77 K in 2-MTHF glass. (c) The results of global fitting obtained from sequential decay path model of TA spectra taken in VIS and in (d) NIR ranges; (e) the representative TA kinetics taken in the VIS and NIR ranges accompanied by fits obtained from global fitting.

state that is generated most probably from the S* state by a singlet fission mechanism [18,34,35].

The bleaching pattern of BChl *a* does not directly mirror the steady-state absorption shape (Fig. 1b). The TA spectra show the split of the B800 band but amplitude ratio of B850 and B800 bleaching features is ~4.0 while the ratio of the steady-state absorption bands is ~1.2. This phenomenon is well-known and has been studied in detail by Kennis and coworkers [9,10,36]. It is a consequence of strong exciton coupling in the B850 ring, resulting in concentration of oscillator strength in the B850 optical transitions.

Global fitting results of both VIS and NIR ranges are given in Fig. 5b. The fitting was performed independently in both spectral ranges. A simple sequential kinetic model does not reflect the complex migration of the absorbed energy within the LH2 complex. Nevertheless by comparison of the effective lifetimes and spectral shapes in the LH2 with their complements obtained for individual carotenoids in 2-MTHF a quite satisfactory model can be constructed. In the VIS range the first four EADS are unambiguously attributed to rhodopin due to their spectral and temporal similarities to those obtained in 2-MTHF. The 0.28 ps EADS is associated with the $S_2(1^1B_u^+)$ state. Previous studies revealed that the lifetime of that state of carotenoid bound into LH2 usually shortens to 50–100 fs due to additional depletion associated with energy transfer to BChl *a* [24,37–39]. Limited instrument time resolution does not allow resolution here of such differences between $S_2(1^1B_u^+)$ state lifetime of carotenoids in 2-MTHF and bound in the LH2. The lifetimes and spectral shapes of 0.45 and 3.7 ps EADS suggest that these components are associated with non-relaxed and relaxed $S_1(2^1A_g^-)$ states, similar to those obtained for rhodopin in 2-MTHF. The effective excited state lifetimes of carotenoids bound to LH2 could be shorter than in solvents due to processes such as energy transfer to other molecules as well can be tuned by the protein environment [40]. The 15 ps EADS component has spectral shape very similar to that observed for the S* state of rhodopin measured in 2-MTHF. However, it has been proposed that in LH2 the S*-like state is a precursor of carotenoid excited

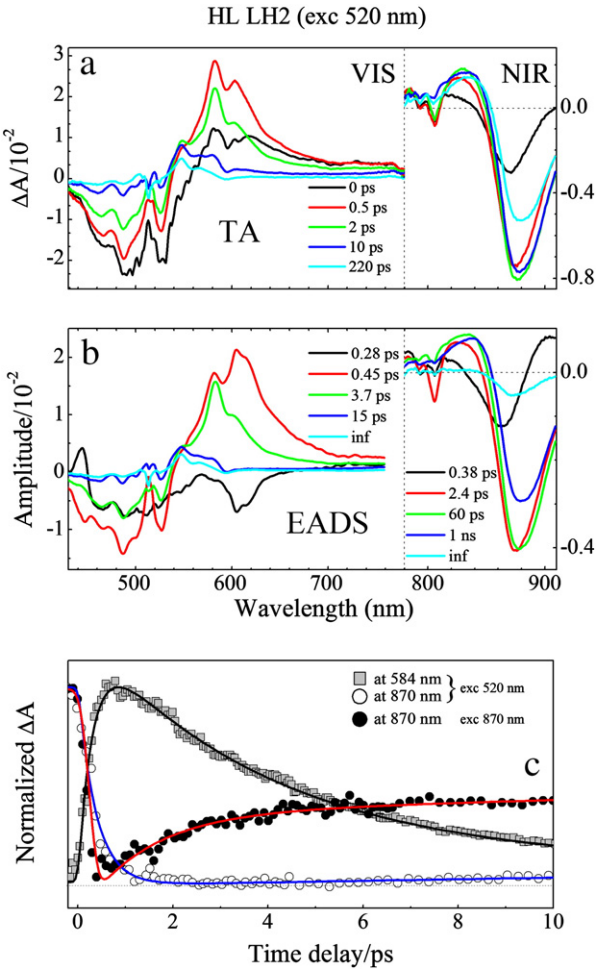

Fig. 5. (a) 77 K transient absorption spectra (TA) of the HL LH2 taken at different delay times, excited at 520 nm; (b) The results of global fitting obtained from sequential decay path model of the TA datasets taken in the VIS and in NIR spectral ranges; (c) The representative TA kinetics taken in the VIS and NIR ranges accompanied by the fits obtained from global fitting. The wavelengths corresponding to the kinetic traces and excitation used are also indicated. The traces were normalized and offset for better comparability.

triplet state [18,34,35]. The excited state transition of the rhodopin triplet state manifests in the infinite EADS.

Fitting results of the TA dataset obtained in the NIR range can be understood as follows: the 0.38 EADSs is associated with decay of the $S_2(1^1B_u^+) \rightarrow S_n$ band (TA transition is partially observed as a positive broad band ~900 nm) coupled with the rise of bleaching of the BChl *a* Q_y band. The 2.4 ps EADS is clearly associated with decay of the B800 bands. There is no noticeable change in amplitudes of B850 between the 2.4 ps and 60 ps EADS. Based on analogy to prior work [41] the 60 ps EADS component is a manifestation of inter-ring annihilation of B850 excitons. Detailed studies of excitation decay in *Rb. sphaeroides* LH2 upon direct B850 excitation performed in various detergent concentrations at RT demonstrated that below a critical micelle concentration complexes form clusters and provide ideal condition for annihilation of the B850 excitons from neighboring rings. Inter-ring annihilation process is indicated by additional fast decay component significantly depleting initial excitons population [41]. The critical micelle concentration of DDM is 0.009% w/v (in water). Despite the fact that the final concentration of DDM in the frozen samples is above that value (0.04%) aggregation may occur in such a mixture due to smaller detergent mobility. In case of the LH2 from *Rb. sphaeroides* time constants of inter-ring annihilation varies from 30 to 50 ps. That is very close to 60 ps obtained here. The EADS with lifetime of 1 ns reflects the decay of the B850 exciton. The spectral shape of the infinitely long lived (on the time scale of the measurements) EADS suggests that a small percentage of BChls end up in the excited triplet state that is formed through intersystem crossing.

Fig. 5c shows representative kinetic traces recorded at 584 nm (maximum of rhodopin $S_1(2^1A_g^-) \rightarrow S_n$ TA band), at 870 nm (bleaching of Q_y band of BChl *a*) upon excitation at 520 nm (rhodopin) and at 870 nm upon direct excitation of BChl *a* (870 nm). The traces are accompanied by fits obtained from global fitting. The time profiles are normalized and offset for better comparability. Difference in the rise of bleaching of the BChl *a* Q_y band is clearly noticeable. While for direct BChl *a* excitation the rise is practically instantaneous (within the laser pulse), in the case of 520 nm excitation the bleaching reaches a minimum at ~2 ps. A similar phenomenon was observed for LH2 from *Rb. sphaeroides* upon spheroidene excitation, which is the carotenoid that is bound into the LH2 in this bacterial species and was interpreted as clear evidence of energy transfer from the $S_1(2^1A_g^-)$ state [18,42]. However, in the case of the LH2 from *Rb. sphaeroides*, the rise of bleaching of BChl *a* Q_y band is significantly longer (the minimum was reached at

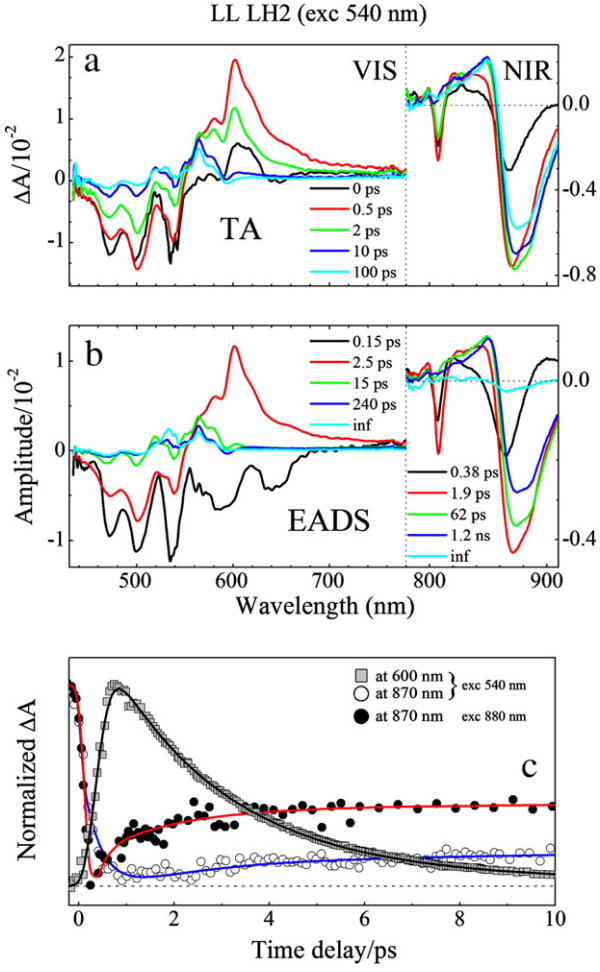

Fig. 6. (a) 77 K transient absorption spectra (TA) of the HL LH2 taken at different delay times, excited at 540 nm; (b) The results of global fitting obtained from sequential decay path model of the TA datasets taken in the VIS and in NIR spectral ranges; (c) The representative TA kinetics taken in the VIS and NIR ranges accompanied by the fits obtained from global fitting. The wavelengths corresponding to the kinetic traces and excitation used are also indicated. The traces were normalized and offset for better comparability.

~9 ps after excitation pulse) and has a very prominent contribution to overall signal.

Fig. 6 shows the TA spectra, global fitting results and representative kinetics of the Sulph-LL LH2 upon excitation at 540 nm, the wavelength that most likely excites anhydrorhodovibrin (and rhodovibrin). The global fitting results of TA dataset taken in the VIS range demonstrate a similar spectral pattern observed for the Thio-HL form. The important remark is that the effective lifetime of the $S_1(2^1A_g^-)$ state of anhydrorhodovibrin shortens from 3.2 ps in 2-MTHF to 2.5 ps in the LH2. In addition, global fitting of the TA dataset in the VIS range revealed an additional long-lived component with time constant of 240 ps that was not present in Thio-HL LH2. Based on the spectral shape of that component, which is almost identical to the infinitive EADS associated with decay of excited triplet state of anhydrorhodopin, the 240 ps kinetic component can be attributed to a pool of extremely fast decaying carotenoid triplets. Global fitting results of TA data from the NIR range show very good agreement with those obtained for Thio-HL LH2. The remarkable difference is observed for the second EADS associated with decay of B800 band. It is shorter by 0.5 ps (1.9 vs. 2.4 ps) compared to its counterpart from Thio-HL LH2.

The representative kinetic traces were recorded at 600 nm (maximum of anhydrorhodovibrin $S_1(2^1A_g^-) \rightarrow S_n$ TA band), at 870 nm (bleaching of Q_y band of BChl *a*) upon excitation at 540 nm (rhodovibrin) and at 870 nm upon direct excitation of BChl *a* (880 nm). The traces are accompanied by fits obtained from global fitting. The time profiles are normalized and offset for better comparability. Difference in the rise of bleaching of the BChl *a* Q_y band is still noticeable but is not so evident such as for Thio-HL LH2. Also, the minimum of BChl *a* Q_y bleaching is reached faster, at ~1.3 ps after excitation. Transient absorption results obtained for the Sulph-LL LH2 excited in its B800 band are shown in Fig. 7. The B800 band bleachings occur instantly upon excitation. Also, a partial bleaching of the B850 band is noticeable. The presence of B850 bleaching is associated with excitation of a weakly allowed higher excitonic band of B850 that overlaps with the Q_y band of monomeric B800 BChls. Bleaching of the B850 band becomes fully developed after few picoseconds. Global fitting results (Fig. 7b) show that B800 band

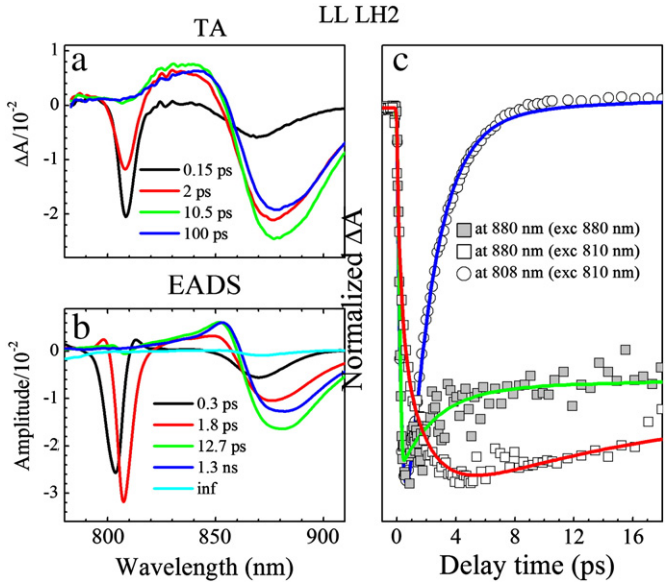

Fig. 7. (a) 77 K transient absorption spectra (TA) of the LL LH2 taken in the NIR spectral range at different delay times upon excitation of B800 band at 810 nm; (b) The results of global fitting obtained from sequential decay path model of the TA datasets and (c) the representative TA kinetic traces accompanied by fits obtained from global fitting. The wavelengths corresponding to the kinetic traces and excitations are also indicated. The traces were normalized for better comparability.

first relaxes with time constant of 0.38 ps (bleaching of Q_y band shifts to longer wavelengths) and then recovers with 1.8 ps time constant and excitation is transferred to B850, to an excited state (exciton) that persists for nanoseconds. The presence of additional intermediate kinetic components (12.7 ps) related to temporal relaxation in the B850 excited state suggests complex decay characteristics that may be related with singlet–singlet annihilation within B850 array in the LH2 ring as well as with inter-complex exciton annihilation [41,43]. The spectral shape of EADS with lifetime of 1.3 ns (compared to 1.2 ns obtained upon excitation of carotenoid) suggests that it is associated with the decay of the B850 exciton. The infinite residual bleach of B850 reflects the fraction of B850 that decays to form in a triplet state by intersystem crossing. The representative kinetics of decay of B800 band (808 nm trace) and rise of B850 band (880 nm trace) are shown in Fig. 7c and allow comparison of the temporal behavior of both BChl *a* forms after excitation of the B800 band and in case of B850 also upon direct excitation. There is a striking difference in a rise of bleaching of B850 band upon direct and B800 excitations. The slow rise of the 880 nm kinetic trace observed in the case of B800 excitation is a clear indication of energy transfer between both forms of BChl *a* in this LH2.

The TA results obtained for the Thio-HL LH2 upon excitation of its B800 sub-bands (792 and 805 nm) are shown in Fig. 8. For simplicity purposes they will be abbreviated as $B800_B$ (792 nm) and $B800_R$ (805 nm) from here on. To assure that sub-bands were excited independently, the 792 nm sub-band was excited at 780 nm while 805 nm sub-band at 810 nm. The excitation at 780 nm results in instantaneous bleach of the $B800_B$ sub-band. The bleaching amplitude is greatest at 100–200 fs after excitation and then decays within a few ps. The decay of the bleached $B800_B$ sub-band is very clearly synchronized with the rise of the bleach of the $B800_R$, suggesting excitation transfer between the $B800_B$ and $B800_R$ BChls. On the other hand, if the $B800_R$ sub-band is excited at 810 nm, the TA spectra indicate that initially this band is almost exclusively bleached with no signature of any bleaching associated with the $B800_B$. The bleaching of $B800_R$ sub-band reaches minimum after a few hundred femtoseconds and then spectrum recovers within a few picoseconds and excitation is transferred to the B850 exciton. The effective excited state lifetime of BChl *a* molecules associated with $B800_B$ sub-band is 1.1 ps while for $B800_R$ it is 2.6 ps.

The results of global fitting of datasets obtained upon direct excitation of the $B800_R$ sub-band (Fig. 8d) revealed that the effective lifetime of the excited state of BChls associated with this absorption signature decays with a time constant of ~1.6 ps, almost twice shorter compared to situation in which $B800_R$ BChl *a* excited state was populated by energy transfer from $B800_B$ (see above). Fig. 8e and f show representative kinetics (normalized) of these events in the Thio-HL LH2 complex in each band. The kinetic trace at 808 nm clearly shows the different temporal behavior when exciting at the two different wavelengths. In the case of 810 nm excitation (into the $B800_R$), the rise of bleaching of the $B800_R$ sub-band (monitored at 808 nm) occurs within the instrument's response, while upon 780 nm excitation (into the $B800_B$) the rise of bleaching of the $B800_R$ sub-band is well-resolved and in addition, is coupled with $B800_B$ excited state decay (monitored at 788 nm).

4. Discussion

4.1. Excitation transfer paths within LH2 complex

Upon the assumption that protein environment does not change carotenoid properties like energies and lifetimes of excited states, the detailed information about lifetimes of excited states of individual carotenoids measured separately and in the LH2 complex allows estimation of the efficiencies of energy transfer to BChl *a*. The correctness of that assumption is somewhat problematic. It is impossible to be certain if 2-MTHF and protein environment will interact with

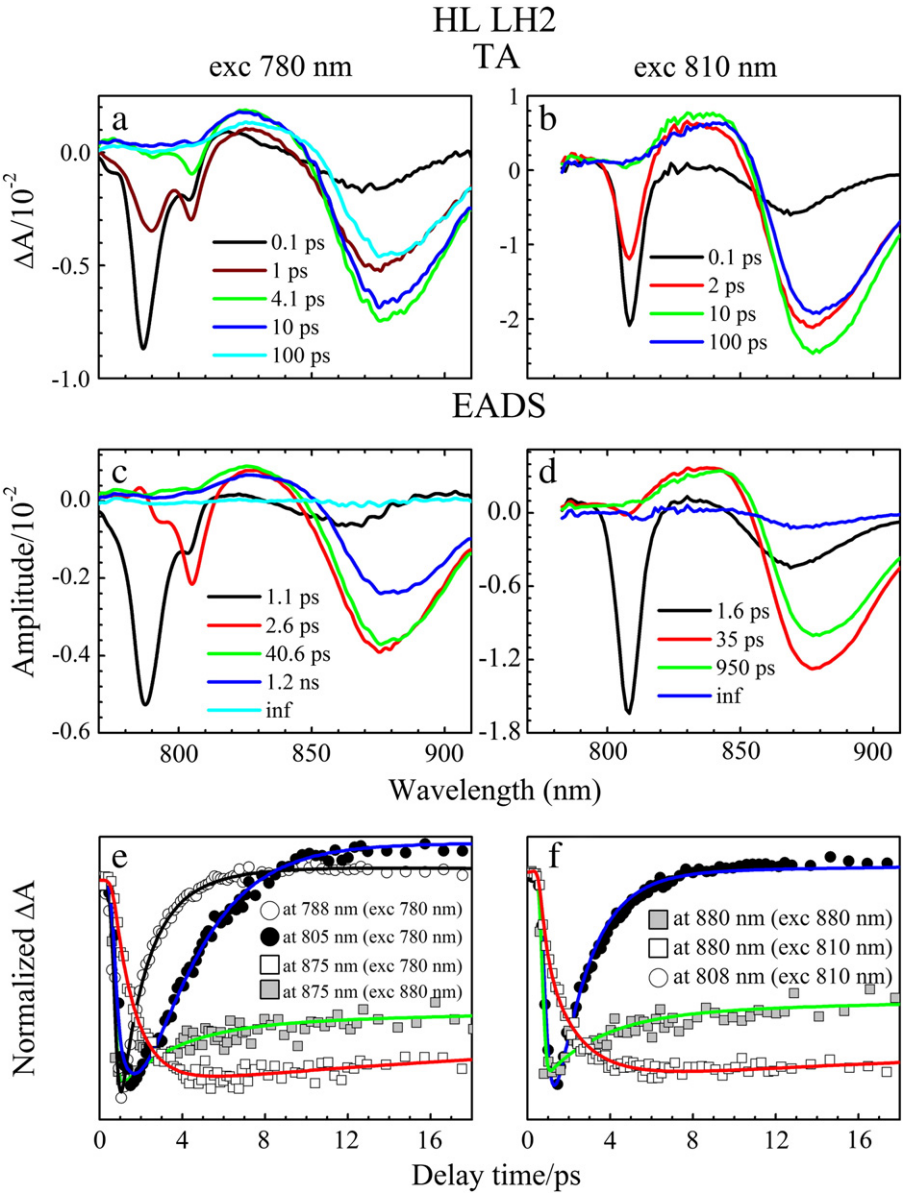

Fig. 8. (a, b) 77 K transient absorption spectra (TA) of the HL LH2 taken in NIR spectral range at different delay times upon excitation of two different peaks of split B800 band; (c, d) The results of global fitting obtained from sequential decay path model of the TA datasets; (e, f) the representative TA kinetics accompanied by fits obtained from global fitting. The wavelengths corresponding to the kinetic traces and excitations are also indicated. The traces were normalized at the minimum to enhance visibility and fit precision.

carotenoid in the same way at 77 K. However, there is a very good agreement between steady-state and time-resolved spectra of measured carotenoids in both surrounds and these indirectly suggest that excited states are affected in a similar way. If so, for each excited state the Car-to-BChl *a*, energy transfer efficiency $\phi_{ET}(S_i)$ can be expressed as:

$$\phi_{ET}(S_i) = \left(1 - \frac{\tau_{Si}^{LH2}}{\tau_{Si}^{SOLV}}\right) \times 100 \quad i = 1,2 \tag{1}$$

where $\tau_{Si}^{LH2}$and $\tau_{Si}^{SOLV}$are the lifetimes of the $S_1(2^1A_g^-)$ and $S_2(1^1B_u^+)$ state in the LH2 and in 2-MTHF at 77 K, respectively. A difference in the $S_1(2^1A_g^-)$ lifetime is clearly observed; however, the ~130 fs temporal resolution of the TA spectrometer does not allow precise measurement of the $S_2(1^1B_u^+)$ excited-state lifetime. Nevertheless, an expected excitation transfer path can be deduced upon the assumption that the overall ϕ_{ET} obtained from steady-state fluorescence spectroscopy and from dynamic analysis should be equal.

For anhydrorhodovibrin ϕ_{ET} (in %) can be calculated from Eq. (2):

$$\phi_{ET} = \phi_{ET}(S_2) + \left(100 - \phi_{ET}(S_2) - \phi_{S_2 \to S^*}(S^*)\right) \times \frac{\phi_{ET}(S_1)}{100} \tag{2}$$

Based on ultrafast rise of the TA signal associated with the S^* state it may be assumed that S^* is formed directly from the $S_2(1^1B_u^+)$ for this molecule. Also, it is assumed that S^* state does not play any significant role in energy transfer to BChl *a* and that its role is limited to being a precursor in triplet formation, in agreement with previous studies [18,24,35]. The percentage of the $S_2(1^1B_u^+)$ state ($\phi_{S_2 \to S^*}(S^*)$) that affords S^* can be calculated from the ratio of bleaching of the ground-state absorption associated with the S^* TA signal to the total ground-state absorption bleaching observed at initial delay time. For anhydrorhodovibrin in the Sulph-LL LH2 the $\phi_{ET}(S_1)$obtained based on

Eq. (1) is 20%. The data becomes consistent with a total $\phi_{ET}=40\%$, obtained from steady-state fluorescence measurements, when $\phi_{ET}(S_2)$ is 30% ($\phi_{S_2\rightarrow S^*}(S^*)$ was estimated to be ~17%). Energy transfer path could be more complicated for rhodopin, a dominant carotenoid in the Thio-HL LH2. It is very probable that in addition to the $S_1(2^1A_g^-)$ and $S_2(1^1B_u^+)$ states, the hot-$S_1(2^1A_g^-)$ state may participate in the energy transfer pathway because the effective lifetime of this state is also shorter in the LH2 than in 2-MTHF. One of simple models that could meet the criterion of total $\phi_{ET}=37\%$ is described by Eq. (3). The model assumes that S* is formed from the non-relaxed $S_1(2^1A_g^-)$ state:

$$\phi_{ET} = \phi_{ET}(S_2) + (100-\phi_{ET}(S_2)-\phi) \times\left(1-\frac{\phi_{hotS_1\rightarrow S^*}(S^*)}{100}\right)\times\frac{\phi_{ET}(S_1)}{100} \quad (3)$$

The agreement is obtained if $\phi_{ET}(S_2)$ is assumed to be 19% (from experimental data $\phi_{ET}(S_1)$ and $\phi_{hotS_1\rightarrow S^*}(S^*)$are 30% and 25%, respectively).

The applied models demonstrate that in both cases the $S_1(2^1A_g^-)$ state should significantly contribute in overall energy transfer. In case of rhodopin it will be near 50%, for anhydrorhodovibrin ~30% of total ϕ_{ET}. If these predictions are correct, Car-to-BChl *a* energy transfer via carotenoid $S_1(2^1A_g^-)$ state should be very clearly manifested by a prominent slow phase rise of bleaching of the B850 band that should account 30–50% of the signal amplitude. Fig. 9 shows normalized kinetic traces of rise and initial decay of bleaching of B850 band monitored at 870 nm upon excitation with different wavelengths. It is apparent that kinetic traces obtained upon 520 and 540 nm excitations do not contain any slow phase rise component as is visible in the case of 810 nm excitation. Most of the bleaching signal is instantaneously formed and comprises extremely fast $S_2(1^1B_u^+)\rightarrow$ BChl *a* energy transfer. The additional small and slightly slower rise component manifested within the first 3 ps is associated with residual B800–B850 energy transfer and was also previously observed for the LH2 from *Rb. sphaeroides* upon excitation to the BChl *a* Q_x band [18]. This undoubtedly shows that even though shortening of the $S_1(2^1A_g^-)$ lifetime is observed it is not related with the energy transfer to BChl *a*. Hence the carotenoids present in the LH2 complexes studied here transfer excitation energy exclusively from their $S_2(1^1B_u^+)$ state. These observations confirm that the $S_1(2^1A_g^-)$ lifetime can be tuned by protein environment, previously observed for xanthophylls that were incorporated into the refolded LHCII apoprotein from maize [40] as well as that carotenoids with carbon-carbon conjugated double bonds *N* of 11 or more are not able to transfer energy to BChl *a* from the $S_1(2^1A_g^-)$ electronic state [44].

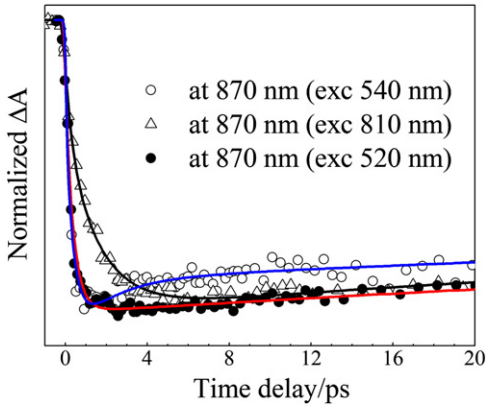

Fig. 9. Kinetic traces representing rise and initial decay of B850 exciton bleaching of HL or LL LH2 upon excitation to 520 nm (rhodopin), 540 nm (rhodovibrin) and 810 nm B800 BChl *a*.

4.2. Carotenoid distribution and light condition of culture growth

It is interesting to ask why this bacterial species completely remodels its carotenoid distribution in the LH2 complexes in response to changes in growth conditions since this causes an almost negligible impact on Car-to-BChl *a* EET. The steady-state absorption and fluorescence excitation measurements show that for the Sulph-LL LH2 Car-to-BChl *a* EET increases only ~2% compared to the Thio-HL form. This value could be easily accounted for by the uncertainties in our analysis. We have performed a simple modeling study in order to investigate this behavior. Fig. 10 illustrates how effective the Sulph-LL and Thio-HL LH2 absorption spectra are in terms of photon capturing. The red and green dotted lines are RT $1-T$ spectra of both complexes normalized in the Soret band. The absorption spectra show that the complexes are identical molecularly—the relative ratio of BChls and carotenoids is the same (similar amplitudes of Soret, Q_x and carotenoid absorptive bands in both complexes); however, interactions between BChls are significantly different in both LH2 complexes. This is clearly visible in the shape of absorption in the NIR (B850 band). The solid blue line (Sun em.) represents the standard reference solar spectrum at ground level (based on AM1.5 global-ASTMG173) in which spectral irradiance was converted to number of photons/m^2 and corrected by absorption of a 5 cm layer of water that is the average depth of the bacterial growth solution in our laboratory conditions. If this spectral irradiance is multiplied by the $1-T$ spectra and integrated the results can show how effective the two LH2 complexes are in photon absorption. The results shown in Fig. 10a reveal that the two LH2 complexes are equally effective for absorption within the carotenoid bands (430–570 nm). This is because the carotenoid absorption bands are very

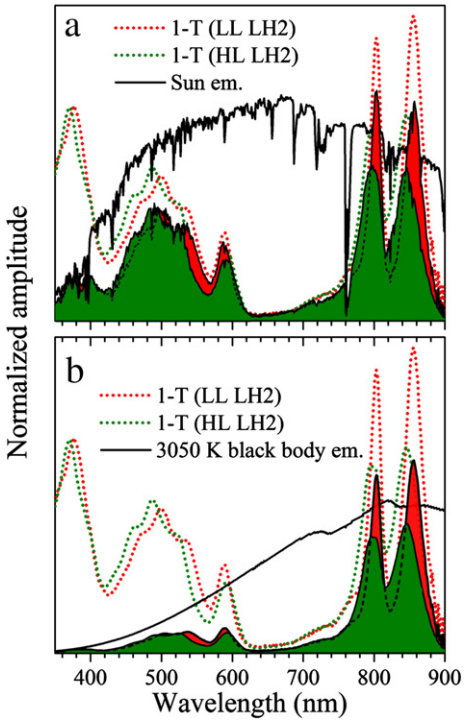

Fig. 10. (blue) Solar light spectrum, (dashed black) emissive spectrum of light source used to grow the bacterium (modeled by 3050 K black body emission), (dashed red) $1-T$ spectrum of the LL LH2 and (dashed green) $1-T$ spectrum HL LH2. The filled profiles are the results of multiplying the $1-T$ spectra by the 3050 K black body emission profile and demonstrate how effectively photons are captured by two forms of the LH2. The spectral irradiance of Sun emission spectrum and black body emission profile was converted to number of photons/m^2 and corrected by absorption of 5 cm layer of water.

close to the peak of the solar irradiation and a small wavelength shift here results in an imperceptible change in the integration results (short-wavelength loss and long-wavelength gain in the spectrum practically compensate).

However, in laboratory conditions the cultures were grown under artificial light. The incandescent bulbs used as light sources have emissive profiles that can be modeled by black body emission with color temperature of 3050 K (here the spectral irradiance was also converted to the number of photons/m^2 and corrected by absorption of 5 cm water layer) (Fig. 10b). The light used to grow the bacteria (black line) has significantly different characteristics from its solar counterpart and in this case the spectral shift of the carotenoid band leads to noticeable differences in number of absorbed photons. The profiles indicated with filled area are the results of multiplying $1-T$ spectra by 3050 K spectrum. In this case the integration results show that carotenoids in the Sulph-LL LH2 can capture ~8% more photons compared to the Thio-HL form. Similar analysis performed for the entire Sulph-LL LH2 absorption spectrum shows that the performance of the Sulph-LL is 12% better than Thio-HL LH2 under laboratory light and ~6% better under Sun light growth. These differences, though small, could be important, especially when light is limiting. It would be of interest to test this idea under natural conditions in the wild.

4.3. Spectral variants of monomeric B800 BChl a within the single LH2

Transient absorption results upon excitation into the B800 BChl *a* provide a definitive answer for the origin of the split of the B800 band in the HL LH2. First of all, if the $B800_B$ and $B800_R$ bands are associated with different excitonic levels of a single B800, excitation of either of the bands should result in simultaneous bleaching of both. This effect is not observed. Secondly, if both bands are associated with BChl *a* species from different LH2 complexes, excitation of the short wavelength form will not cause so rapid energy transfer to the long-wavelength form due to spatial separations (BChls are in different proteins); the inter-protein energy transfer between aggregated LH2 proteins was shown to have time constants of ~60 ps. However, the TA and global fitting results clearly demonstrate that following excitation of $B800_B$ there is direct and fast (~2 ps) energy transfer to the $B800_R$ band, seen as a delayed development of bleaching of this band (blue line in Fig. 8e). Hence both spectral bands must originate from a ground state absorption of two different monomeric BChl *a* species distributed within a single LH2 complex. For a B800 molecule ($B800_B$) that possesses a neighbor with a long-wavelength character ($B800_R$) two deactivation pathways are possible $B800_B \rightarrow B800_R$ and $B800_B \rightarrow B850$. The $B800 \rightarrow B850$ energy transfer lifetime was experimentally measured (also here) for a number of different LH2 complexes and has a value of ~1.2–1.6 ps at 77 K [45–49] and was accounted by resonant transfer involving a weakly allowed band of a B850 exciton overlapping with B800 emission (see [50] for extensive review). The $B800 \rightarrow B800$ inter-molecule (or intra-band) energy transfer had been also extensively studied in LH2 complexes from non-sulfur bacterial species (no B800 split) using various experimental techniques like photon echo and hole burning as well theoretical studies. The estimates from these studies place value of the $B800 \rightarrow B800$ energy transfer time constant in range between 500 fs and 1 ps [9,37,48,51–54] . It may be assumed that in terms of BChl *a* pigment organization, the structures of the LH2 complexes studied here have substantial analogy to their counterparts from the non-sulfur bacteria and distances between BChl *a* and orientations between their transition dipoles are preserved. Therefore, a similar value of time constant for B800 intra-molecular energy transfer is expected. Upon such assumption the effective lifetime of the $B800_B$ (inverse of sum of $B800_B \rightarrow B800_R$ and $B800_B \rightarrow B850$ transfer rates) should shorten to ~620 fs. The global fitting results (Fig. 8c) demonstrate that the situation in the studied LH2 is not so simple. The effective lifetime of $B800_B$ is 1.1 ps. The branching pattern ratio ($B800_B \rightarrow B800_R$ and $B800_B \rightarrow B850$) can be elucidated from the proportion of amplitudes of bleaching of the B800 sub-bands (Fig. 8a). Bleaching of the $B800_R$ band reaches only 40% of bleaching of $B800_B$ band. Upon the assumption that B800 comprises the same number of spectral variants of BChl *a* (due to similar amplitudes of both peaks in the steady-state absorption spectrum) only 40% of the excitation is transferred from $B800_B$ to $B800_R$, the remaining 60% is transferred directly to the B850 exciton. Simple conversion of the 1.1 ps effective lifetime to the rate constant and knowledge of the branching pattern allows calculating the $B800_B \rightarrow B800_R$ and $B800_B \rightarrow B850$ energy transfer rates and time constants. It points out that the $B800_B \rightarrow B800_R$ energy transfer time constant is 2.8 ps while $B800_B \rightarrow B850$ is 1.8 ps. It is very probable that the observed 2.8 ps (in LH2 studied here) vs. 1.0 ps (in LH2 from non-sulfur photosynthetic bacteria) difference can be accounted by change in the spectral overlap between $B800_B$ fluorescence and $B800_R$ absorption compared to their complements from LH2s having no B800 split (better overlap).

5. Conclusions

A change of distribution of the carotenoids in the Sulph-LL LH2 complex modifies the absorptive properties of the LH2 antenna complex to maintain maximum photon capture performance upon suppressed light condition. However, this change cannot be definitively attributed to a simple response to light conditions because both cultures were grown in media having different sulfur sources and not all growth conditions were constant. The overarching finding is that B800 band split origins from two spectrally distinct BChl *a* molecules bound within the same B800-type BChl *a* ring in the LH2 complex.

Acknowledgments

This research was supported as a part of the Photosynthetic Antenna Research Center (PARC), an Energy Frontier Research Center funded by the DOE, Office of Science, Office of Basic Energy Sciences under Award Number DE-SC 0001035. Bacterial growth and LH2s preparation by R.J.C. was supported by *BBSRC*.

References

[1] G. McDermott, S.M. Prince, A.A. Freer, A.M. Hawthornthwaitelawless, M.Z. Papiz, R.J. Cogdell, N.W. Isaacs, Crystal structure of an integral membrane light-harvesting complex from photosynthetic bacteria, Nature 374 (1995) 517–521.
[2] S.M. Prince, M.Z. Papiz, A.A. Freer, G. McDermott, A.M. Hawthornthwaite-Lawless, R.J. Cogdell, N.W. Isaacs, Apoprotein structure in the LH2 complex from *Rhodopseudomonas acidophila* strain 10050: modular assembly and protein pigment interactions, J. Mol. Biol. 268 (1997) 412–423.
[3] M.Z. Papiz, S.M. Prince, T. Howard, R.J. Cogdell, N.W. Isaacs, The structure and thermal motion of the B800-850 LH2 complex from *Rps. acidophila* at 2.0Å resolution and 100 K: New structural features and functionally relevant motions, J. Mol. Biol. 326 (2003) 1523–1538.
[4] J. Koepke, X. Hu, C. Muenke, K. Schulten, H. Michel, The crystal structure of the light-harvesting complex II (B800-850) from *Rhodospirillum molischianum*, Structure 4 (1996) 581–597.
[5] G. Britton, S. Liaaen-Jensen, H. Pfander, Carotenoids Handbook, in: Carotenoids, Birkhäuser Basel, Basel, Boston, Berlin, 2004.
[6] S. Kereiche, L. Bourinet, W. Keegstra, A.A. Arteni, J.M. Verbavatz, E.J. Boekema, B. Robert, A. Gall, The peripheral light-harvesting complexes from purple sulfur bacteria have different 'ring' sizes, FEBS Lett. 582 (2008) 3650–3656.
[7] B. van Dijk, T. Nozawa, A.J. Hoff, The B800-850 complex of the purple bacterium *Chromatium tepidum*: low-temperature absorption and Stark spectra, Spectrochim. Acta A 54 (1998) 1269–1278.
[8] D. Garcia, P. Parot, A. Vermeglio, M.T. Madigan, The light-harvesting complexes of a thermophilic purple sulfur photosynthetic bacterium *Chromatium tepidum*, Biochim. Biophys. Acta 850 (1986) 390–395.
[9] J.T.M. Kennis, A.M. Streltsov, S.I.E. Vulto, T.J. Aartsma, T. Nozawa, J. Amesz, Femtosecond dynamics in isolated LH2 complexes of various species of purple bacteria, J. Phys. Chem. B 101 (1997) 7827–7834.
[10] J.T.M. Kennis, A.M. Streltsov, T.J. Aartsma, T. Nozawa, J. Amesz, Energy transfer and exciton coupling in isolated B800–850 complexes of the photosynthetic purple sulfur bacterium *Chromatium tepidum*. The effect of structural symmetry on bacteriochlorophyll excited states, J. Phys. Chem. 100 (1996) 2438–2442.

[11] H. Zuber, R.J. Cogdell, Structure and organization of purple bacterial antenna complexes, in: R.E. Blankenship, M.T. Madigan, C.E. Bauer (Eds.), Anoxygenic Photosynthetic Bacteria, Kluwer Academic Publishers, Dordrecht., 1995, pp. 315–348.
[12] H. Hayashi, T. Nozawa, M. Hatano, S. Morita, Circular dichroism of bacteriochlorophyll a in light harvesting bacteriochlorophyll protein complexes from *Chromatium vinosum*, J. Biochem. 89 (1981) 1853–1861.
[13] K.A. Malik, A modified method for the cultivation of phototrophic bacteria, J. Microbiol. Methods (1983) 343–352.
[14] I.H. van Stokkum, D.S. Larsen, R. van Grondelle, Global and target analysis of time-resolved spectra, Biochim. Biophys. Acta 1657 (2004) 82–104.
[15] D.M. Niedzwiedzki, M. Fuciman, M. Kobayashi, H.A. Frank, R.E. Blankenship, Ultrafast time-resolved spectroscopy of the light-harvesting complex 2 (LH2) from the photosynthetic bacterium *Thermochromatium tepidum*, Photosynth. Res. 110 (2011) 49–60.
[16] D.M. Niedzwiedzki, D.J. Sandberg, H. Cong, M.N. Sandberg, G.N. Gibson, R.R. Birge, H.A. Frank, Ultrafast time-resolved absorption spectroscopy of geometric isomers of carotenoids, Chem. Phys. 357 (2009) 4–16.
[17] H. Okamoto, M. Ogura, T. Nakabayashi, M. Tasumi, Sub-picosecond excited-state dynamics of a carotenoid (spirilloxanthin) in the light-harvesting systems of *Chromatium vinosum*. Relaxation process from the optically allowed S_2 state, Chem. Phys. 236 (1998) 309–318.
[18] E. Papagiannakis, J.T. Kennis, I.H. van Stokkum, R.J. Cogdell, R. van Grondelle, An alternative carotenoid-to-bacteriochlorophyll energy transfer pathway in photosynthetic light harvesting, Proc. Natl. Acad. Sci. U. S. A. 99 (2002) 6017–6022.
[19] J.P. Zhang, T. Inaba, Y. Watanabe, Y. Koyama, Excited-state dynamics among the $1B_u^+$, $1B_u^-$ and $2A_g^-$ states of all-*trans*-neurosporene as revealed by near-infrared time-resolved absorption spectroscopy, Chem. Phys. Lett. 332 (2000) 351–358.
[20] M. Yoshizawa, D. Kosumi, M. Komukai, H. Hashimoto, Ultrafast optical responses of three-level systems in beta-carotene: resonance to a high-lying $n^1A_g^-$ excited state, Laser Phys. 16 (2006) 325–330.
[21] T. Polivka, V. Sundstrom, Ultrafast dynamics of carotenoid excited states-from solution to natural and artificial systems, Chem. Rev. 104 (2004) 2021–2071.
[22] T. Polivka, D. Zigmantas, H.A. Frank, J.A. Bautista, J.L. Herek, Y. Koyama, R. Fujii, V. Sundstrom, Near-infrared time-resolved study of the S_1 state dynamics of the carotenoid spheroidene, J. Phys. Chem. B 105 (2001) 1072–1080.
[23] D.M. Niedzwiedzki, M.M. Enriquez, A.M. Lafountain, H.A. Frank, Ultrafast time-resolved absorption spectroscopy of geometric isomers of xanthophylls, Chem. Phys. 373 (2010) 80–89.
[24] E. Papagiannakis, I.H. van Stokkum, M. Vengris, R.J. Cogdell, R. van Grondelle, D.S. Larsen, Excited-state dynamics of carotenoids in light-harvesting complexes. 1. Exploring the relationship between the S_1 and S^* states, J. Phys. Chem. B 110 (2006) 5727–5736.
[25] H. Cong, D.M. Niedzwiedzki, G.N. Gibson, A.M. LaFountain, R.M. Kelsh, A.T. Gardiner, R.J. Cogdell, H.A. Frank, Ultrafast time-resolved carotenoid to-bacteriochlorophyll energy transfer in LH2 complexes from photosynthetic bacteria, J. Phys. Chem. B 112 (2008) 10689–10703.
[26] H. Cong, D.M. Niedzwiedzki, G.N. Gibson, H.A. Frank, Ultrafast time-resolved spectroscopy of xanthophylls at low temperature, J. Phys. Chem. B 112 (2008) 3558–3567.
[27] D. Niedzwiedzki, J.F. Koscielecki, H. Cong, J.O. Sullivan, G.N. Gibson, R.R. Birge, H.A. Frank, Ultrafast dynamics and excited state spectra of open-chain carotenoids at room and low temperatures, J. Phys. Chem. B 111 (2007) 5984–5998.
[28] C.C. Gradinaru, J.T. Kennis, E. Papagiannakis, I.H. van Stokkum, R.J. Cogdell, G.R. Fleming, R.A. Niederman, R. van Grondelle, An unusual pathway of excitation energy deactivation in carotenoids: singlet-to-triplet conversion on an ultrafast timescale in a photosynthetic antenna, Proc. Natl. Acad. Sci. U. S. A. 98 (2001) 2364–2369.
[29] D.S. Larsen, E. Papagiannakis, I.H.M. van Stokkum, M. Vengris, J.T.M. Kennis, R. van Grondelle, Excited state dynamics of beta-carotene explored with dispersed multi-pulse transient absorption, Chem. Phys. Lett. 381 (2003) 733–742.
[30] W. Wohlleben, T. Buckup, J.L. Herek, R.J. Cogdell, M. Motzkus, Multichannel carotenoid deactivation in photosynthetic light harvesting as identified by an evolutionary target analysis, Biophys. J. 85 (2003) 442–450.
[31] W. Wohlleben, T. Buckup, H. Hashimoto, R.J. Cogdell, J.L. Herek, M. Motzkus, Pump-deplete-probe spectroscopy and the puzzle of carotenoid dark states, J. Phys. Chem. B 108 (2004) 3320–3325.
[32] H.H. Billsten, J. Pan, S. Sinha, T. Pascher, V. Sundstrom, T. Polivka, Excited-state processes in the carotenoid zeaxanthin after excess energy excitation, J. Phys. Chem. A 109 (2005) 6852–6859.
[33] Z.D. Pendon, G.N. Gibson, I. van der Hoef, J. Lugtenburg, H.A. Frank, Effect of isomer geometry on the steady-state absorption spectra and femtosecond time-resolved dynamics of carotenoids, J. Phys. Chem. B 109 (2005) 21172–21179.
[34] A.E. Jailaubekov, S.H. Song, M. Vengris, R.J. Cogdell, D.S. Larsen, Using narrowband excitation to confirm that the S^* state in carotenoids is not a vibrationally-excited ground state species, Chem. Phys. Lett. 487 (2010) 101–107.
[35] E. Papagiannakis, S.K. Das, A. Gall, I.H.M. van Stokkum, B. Robert, R. van Grondelle, H.A. Frank, J.T.M. Kennis, Light harvesting by carotenoids incorporated into the B850 light-harvesting complex from *Rhodobacter sphaeroides* R-26.1: excited-state relaxation, ultrafast triplet formation, and energy transfer to bacteriochlorophyll, J. Phys. Chem. B 107 (2003) 5642–5649.
[36] J.T.M. Kennis, A.M. Streltsov, H. Permentier, T.J. Aartsma, J. Amesz, Exciton coherence and energy transfer in the LH2 antenna complex of *Rhodopseudomonas acidophila* at low temperature, J. Phys. Chem. B 101 (1997) 8369–8374.
[37] B.P. Krueger, G.D. Scholes, R. Jimenez, G.R. Fleming, Electronic excitation transfer from carotenoid to bacteriochlorophyll in the purple bacterium *Rhodopseudomonas acidophila*, J. Phys. Chem. B 102 (1998) 2284–2292.
[38] A.N. Macpherson, J.B. Arellano, N.J. Fraser, R.J. Cogdell, T. Gillbro, Efficient energy transfer from the carotenoid S_2 state in a photosynthetic light-harvesting complex, Biophys. J. 80 (2001) 923–930.
[39] Y. Koyama, F.S. Rondonuwu, R. Fujii, Y. Watanabe, Light-harvesting function of carotenoids in photo-synthesis: the roles of the newly found 1(1)Bu- state, Biopolymers 74 (2004) 2–18.
[40] T. Polivka, D. Zigmantas, V. Sundstrom, E. Formaggio, G. Cinque, R. Bassi, Carotenoid S-1 state in a recombinant light-harvesting complex of photosystem II, Biochemistry 41 (2002) 439–450.
[41] A. Schubert, A. Stenstam, W.J.D. Beenken, J.L. Herek, R. Cogdell, T. Pullerits, V. Sundstrom, In vitro self-assembly of the light harvesting pigment-protein LH2 revealed by ultrafast spectroscopy and electron microscopy, Biophys. J. 86 (2004) 2363–2373.
[42] T. Polivka, D. Niedzwiedzki, M. Fuciman, V. Sundstrom, H.A. Frank, Role of B800 in carotenoid-bacteriochlorophyll energy and electron transfer in LH2 complexes from the purple bacterium *Rhodobacter sphaeroides*, J. Phys. Chem. B 111 (2007) 7422–7431.
[43] G. Trinkunas, J.L. Herek, T. Polivka, V. Sundstrom, T. Pullerits, Exciton delocalization probed by excitation annihilation in the light-harvesting antenna LH2, Phys. Rev. Lett. 86 (2001) 4167–4170.
[44] T. Polivka, D. Zigmantas, J.L. Herek, Z. He, T. Pascher, T. Pullerits, R.J. Cogdell, H.A. Frank, V. Sundstrom, The carotenoid S_1 state in LH2 complexes from purple bacteria *Rhodobacter sphaeroides* and *Rhodopseudomonas acidophila*: S_1 energies, dynamics, and carotenoid radical formation, J. Phys. Chem. B 106 (2002) 11016–11025.
[45] H.M. Wu, S. Savikhin, N.R.S. Reddy, R. Jankowiak, R.J. Cogdell, W.S. Struve, G.J. Small, Femtosecond and hole-burning studies of B800's excitation energy relaxation dynamics in the LH2 antenna complex of *Rhodopseudomonas acidophila* (strain 10050), J. Phys. Chem. 100 (1996) 12022–12033.
[46] J.L. Herek, N.J. Fraser, T. Pullerits, P. Martinsson, T. Polivka, H. Scheer, R.J. Cogdell, V. Sundstrom, B800 -> B850 energy transfer mechanism in bacterial LH2 complexes investigated by B800 pigment exchange, Biophys. J. 78 (2000) 2590–2596.
[47] G.D. Scholes, G.R. Fleming, On the mechanism of light harvesting in photosynthetic purple bacteria: B800 to B850 energy transfer, J. Phys. Chem. B 104 (2000) 1854–1868.
[48] T. Pullerits, S. Hess, J.L. Herek, V. Sundstrom, Temperature dependence of excitation transfer in LH2 of *Rhodobacter sphaeroides*, J. Phys. Chem. B 101 (1997) 10560–10567.
[49] Y.Z. Ma, R.J. Cogdell, T. Gillbro, Energy transfer and exciton annihilation in the B800–850 antenna complex of the photosynthetic purple bacterium *Rhodopseudomonas acidophila* (Strain 10050). A femtosecond transient absorption study, J. Phys. Chem. B 101 (1997) 1087–1095.
[50] V. Sundstrom, T. Pullerits, R. van Grondelle, Photosynthetic light-harvesting: reconciling dynamics and structure of purple bacterial LH2 reveals function of photosynthetic unit, J. Phys. Chem. B 103 (1999) 2327–2346.
[51] H.M. Wu, N.R.S. Reddy, R.J. Cogdell, C. Muenke, H. Michel, G.J. Small, A comparison of the LH2 antenna complex of three purple bacteria by hole burning and absorption spectroscopies, Mol. Cryst. Liq. Cryst. A 291 (1996) 163–173.
[52] R. Monshouwer, R. van Grondelle, Excitations and excitons in bacterial light-harvesting complexes, Biochim. Biophys. Acta, Bioenerg. 1275 (1996) 70–75.
[53] R. Agarwal, M. Yang, Q.H. Xu, G.R. Fleming, Three pulse photon echo peak shift study of the B800 band of the LH2 complex of *Rps. acidophila* at room temperature: a coupled master equation and nonlinear optical response function approach, J. Phys. Chem. B 105 (2001) 1887–1894.
[54] J.M. Salverda, F. van Mourik, G. van der Zwan, R. van Grondelle, Energy transfer in the B800 rings of the peripheral bacterial light-harvesting complexes of *Rhodopseudomonas acidophila* and *Rhodospirillum molischianum* studied with photon echo techniques, J. Phys. Chem. B 104 (2000) 11395–11408.